Effect of Unfavorable Continuous Phase Density Gradient on Axial Mixing

Timothy L. Holmes and Andrew E. Karr
Otto H. York Co., Inc., Parsippany, NJ 07054

Malcolm H. I. Baird
McMaster University, Chemical Engineering Dept., Hamilton, Ontario, Canada L8S 4L7

Field experience with several industrial reciprocating plate liquid-liquid extraction columns indicated that large density gradients in the continuous phase resulted in excessive backmixing. Since there are no published data on the effect of higher density in the upper section compared to lower density in the bottom section of the column, experiments were performed with the calcium chloride brine-water system in a 76.2 mm diameter reciprocating plate column.

Axial dispersion coefficients, E, were found to be 10–20 times higher than the values in systems with uniform densities. E decreased with increasing agitation to 30% of the value with no agitation. The effect of increasing flow rate of water up the column was to increase both E and the Peclet number. E was correlated with the density difference between any point in the column and tap water. Another correlation was obtained showing the effects of buoyant and mechanical energy input on axial dispersion.

Introduction

It has long been recognized that axial mixing reduces the effectiveness of countercurrent contactors. The effect is particularly noticeable in extraction columns, which operate at relatively low superficial velocities. The equations for the concentration profiles in the presence of axial mixing were developed by Sleicher (1959, 1960), Miyauchi and Vermeulen (1963), and Hartland and Mecklenburgh (1966). Pratt (1975) introduced a simplified design procedure to estimate the height of a contactor for given flow rates and mass transfer performance, under conditions of axial mixing.

In order to apply these calculation methods, it is necessary to have values of the axial dispersion coefficient, E, for each phase. Pratt and Baird (1983) have reviewed previous work on the factors that determine axial dispersion coefficients in various types of extraction column. These factors include:

- Flow rates of each liquid phase
- Column geometry, such as packing or plate design
- Agitation, such as rotation or reciprocation
- Hydraulic nonuniformity effects (which tend to increase with column diameter).

A factor that has not been studied is the presence of an adverse density gradient in the continuous phase. Such a gradient could possibly occur, for example, in the extraction of a heavy metal in high concentrations from an aqueous phase fed to the top of the column and contacted with an organic extractant solution. Although no such effects have been positively identified, it is possible that they may occur in combination with other factors listed above.

Field experience with several production-scale, reciprocating plate liquid-liquid extraction columns handling high concentrations of organic compounds indicated that large adverse density gradients in the continuous phase resulted in excessive backmixing. There are no published data on the effect of a higher density in the upper section as compared to a lower density in the bottom section of the column. Therefore, we decided to obtain such axial mixing data in a 7.62 cm dia. reciprocating plate column of the type developed by Karr (1959). This type of column has achieved extensive industrial application in diameters up to 1.7 m. Axial mixing data in Karr columns of 5.1 and 15.3 cm dia. have been reported respectively by Kim and Baird (1976) and Hafez et al. (1979). More recently, Karr et al. (1987) measured axial mixing in a 50.8 cm dia. column (single-phase conditions only). They also related the scale effect upon axial mixing to the previously

Correspondence concerning this paper should be addressed to M. H. I. Baird.

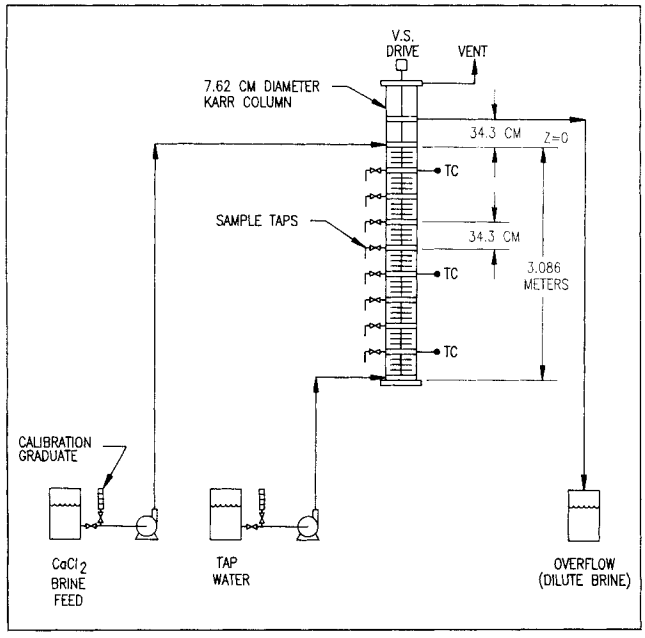

Figure 1. Extraction pilot plant.

developed expression for the effect of diameter upon mass transfer performance (Karr and Lo, 1971, 1979).

System Investigated

In the present paper, axial mixing in a 7.62 cm dia. Karr column was investigated by performing single-phase pilot plant experiments with the $CaCl_2$ brine-water system. The measured density of aqueous $CaCl_2$ solutions at the pilot-plant operating temperature (23°C) was plotted as a function of wt. % hydrated $CaCl_2$ ($CaCl_2 \cdot 2H_20$; data available on microfilm as supplementary material.) Measured refractive indices of aqueous $CaCl_2$ solutions, referred to as brine, at 20°C were also plotted against composition (available in the supplementary material). Brine solutions were prepared by dissolving technical grade $CaCl_2$ beads in tap water to yield, typically, a 44 wt. % hydrated calcium chloride stock solution.

Pilot Plant

Equipment

A simplified diagram of the extraction pilot plant is shown in Figure 1. This pilot plant contained a 7.62 cm dia. glass Karr column with a 3.086 m plate stack and eight sample taps at 34.3 cm intervals along the column; a variable-speed column drive so the agitation frequency could be varied; brine feed and tap water supply and metering systems; and a 1.905 cm dia. overflow line for removing dilute brine from the column. Extraction column temperatures were measured with iron-constantan thermocouples, labeled *TC*, at three locations as shown in Figure 1.

A 316 SS plate stack was used in these experiments. This plate stack contained 1.57 mm thick perforated plates on either 2.7 or 5.24 cm spacing and each plate had an effective free area of 57%. The holes in these plates were 12.7 mm in diameter.

Operating procedure

In the operation of this pilot plant, the tap water flow rate was set at the desired value and the column was filled with water. When the column was full, the agitator was turned on and then the brine feed flow was set at the desired rate. After the entire contents of the extraction column had been displaced four times, a set of steady-state concentration profile samples was taken. The refractive index of each of these samples was measured and converted with the aid of the composition plots to yield the $CaCl_2$ concentration profiles. The density of some of these samples was measured so that the brine concentration could also be determined from the density-composition plot.

In all of the test runs, the brine and tap water volumetric flow rates were equal. Tests with both 44 and 24 wt. % brine feeds were considered. A summary of the conditions investigated with the pilot plant may be seen in Table 1.

Results

Typical concentration profiles, obtained with the 44 wt. % brine feed, may be seen in Figure 2. The most significant backmixing occurred at 0 rpm and as the agitation frequency was increased the axial mixing decreased. A second variable which helped to reduce axial mixing was the superficial water upflow velocity, Figures 2a,b,d. At 0 rpm and $U = 0.658$ cm/s the brine only mixed to $z = -158$ cm, whereas the 0 rpm and $U = 0.165$ cm/s, a significant brine concentration was observed near the bottom of the column ($z = -274.3$ cm). As is shown later, although the axial dispersion coefficient at the higher flow rate is greater than that at the lower rate, the Peclet number, *Pe*, at the high rate is higher than it is at the lower rate, which accounts for the observed differences in concentration profiles.

Table 1. Conditions Investigated with 7.62 cm Dia. Karr Column

Plate Spacing cm	Flow Rate, mL/min			Agitation*									
				44% Brine Feed Runs rpm					24% Brine Feed Runs rpm				
	Brine	Water	U_1 cm/s										
5.24	450	450	0.165	0	50	100	200	300	0	50	100	200	300
5.24	900	900	0.329	0	50	100	200	300	0	50	100	—	300
5.24	1,800	1,800	0.658	0	50	100	200	300	0	50	100	200	300
2.70	450	450	0.165	0	—	100	—	—	0	79	100	200	—
2.70	900	900	0.329	0	79	100	—	—	0	79	100	200	—
2.70	1,800	1,800	0.658	0	—	—	—	—	0	79	100	—	—

*A 1.905 cm agitation stroke was used in all runs.

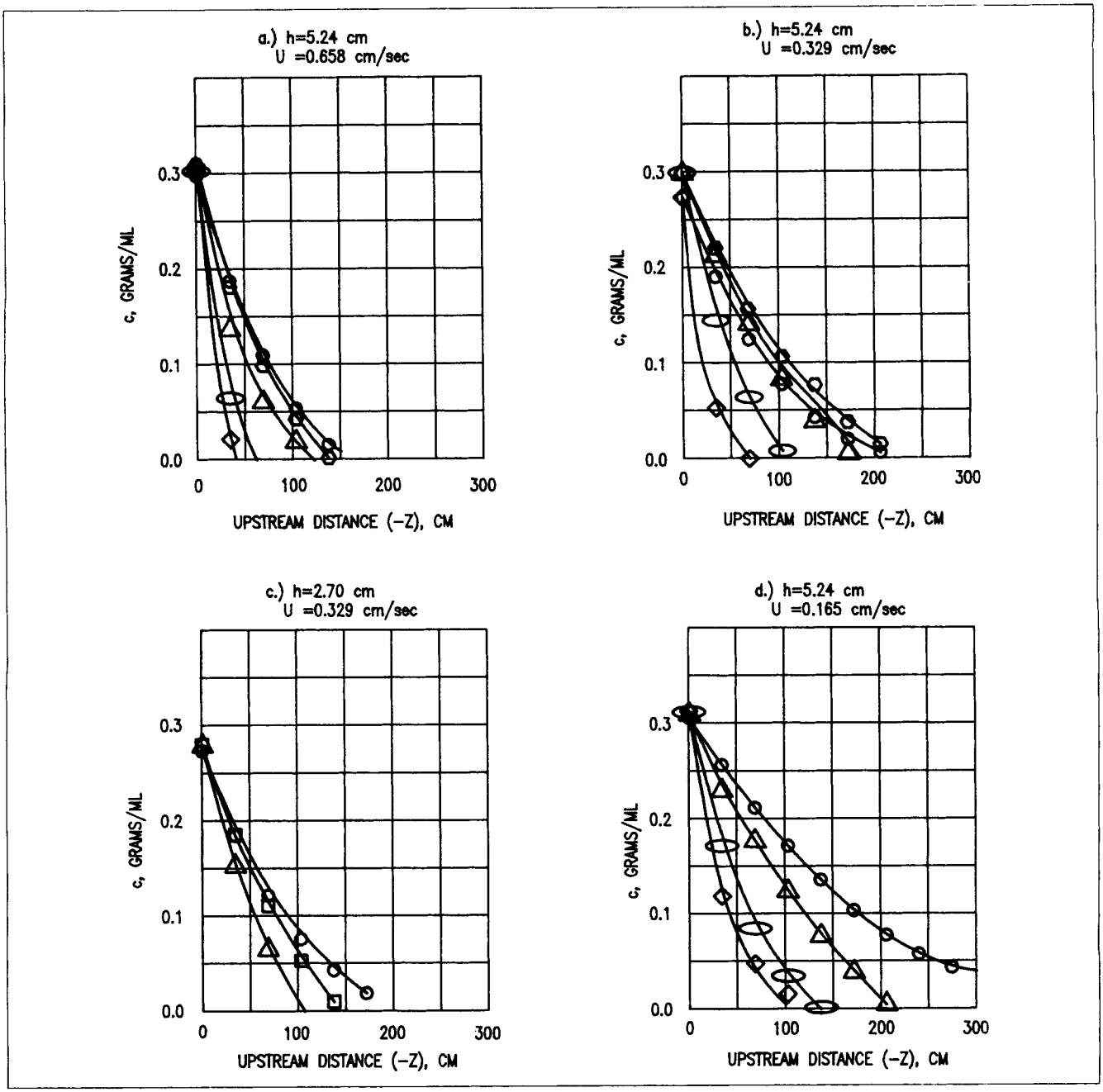

Figure 2. Calcium chloride concentration profiles at different plate spacings and superficial velocities.

Agitation speed, rpm: 0 50 79 100 200 300; Symbol: o o □ △ ⬭ ◇

The effect of plate spacing on axial mixing may be seen by comparing Figures 2b and 2c. At 100 rpm, the brine concentration approached 0 at $z = -175$ cm with 5.24 cm spacing and it approached 0 at $z = -102$ cm with 2.70 cm spacing, so that backmixing is reduced when more plates are included in the stack.

The axial dispersion coefficient, E, was calculated from the steady-state concentration profiles with the following differential material balance equation, originally described by Mar and Babb (1959):

$$cU = E\left(\frac{dc}{dz}\right) \tag{1}$$

Rearranging Eq. 1 yields

$$E = \frac{cU}{dc/dz} \tag{2}$$

In this work E varied throughout the column, unlike the as-

sumptions usually made in axial mixing studies. The concentration gradients were determined graphically from smoothed profile curves drawn through the data points plotted as concentration vs. upstream distance, z. Because the solution density is changing with respect to z, the velocity U is not constant. A total material balance between the entry point of water (superficial velocity U_1, density ρ_o) and any point at $z(<o)$ gives

$$U_1\rho_o = U\rho - E\left(\frac{dc}{dz}\right) \tag{3}$$

Combining this with Eq. 1 gives

$$U = U_1\left(\frac{\rho_o}{\rho - c}\right) \tag{4}$$

The brine density can be written with reasonable accuracy as

$$\rho = \rho_o + 0.7c \tag{5}$$

Hence from Eq. 4,

$$U = \frac{U_1}{1 - 0.3c/\rho_o} \tag{6}$$

At the highest concentrations observed in the column, 300 g/L, the velocity correction is approximately 10%. At most points on the concentration profile, it was considerably less than this.

Axial dispersion coefficients were calculated with Eqs. 1 and 6 and graphically determined dc/dz values. Results of these calculations have been tabulated (available in the supplementary material).

Discussion

Although the axial dispersion coefficients discussed above are based upon slope measurements of smoothed curves drawn through the data and are therefore subject to uncertainty, especially at the highest and lowest concentrations, they do illustrate that E is not constant, and that it increases with density gradient. The magnitudes of E are significantly greater than those reported (Kim and Baird, 1976; Hafez et al., 1979) for uniform-density fluids in which E is typically in the range of 1 to 3 cm^2/s, (50.8 to 152.4 mm dia. columns).

The dependence of E upon density gradient may be characterized by defining an overall density difference, $\Delta\rho$, which is the difference between the local density at any point in the column and the density of pure water, that is,

$$\Delta\rho = \rho - \rho_o \tag{7}$$

where $\rho_o = 0.997$ g/mL. Plots of E vs. $\Delta\rho$ for each of the test runs are shown in Figures 3 and 4. The straight lines on these log-log plots all have a slope of 1/2 and represent a visual fit of the data. In view of this

$$E\alpha\Delta\rho^{1/2} \tag{8}$$

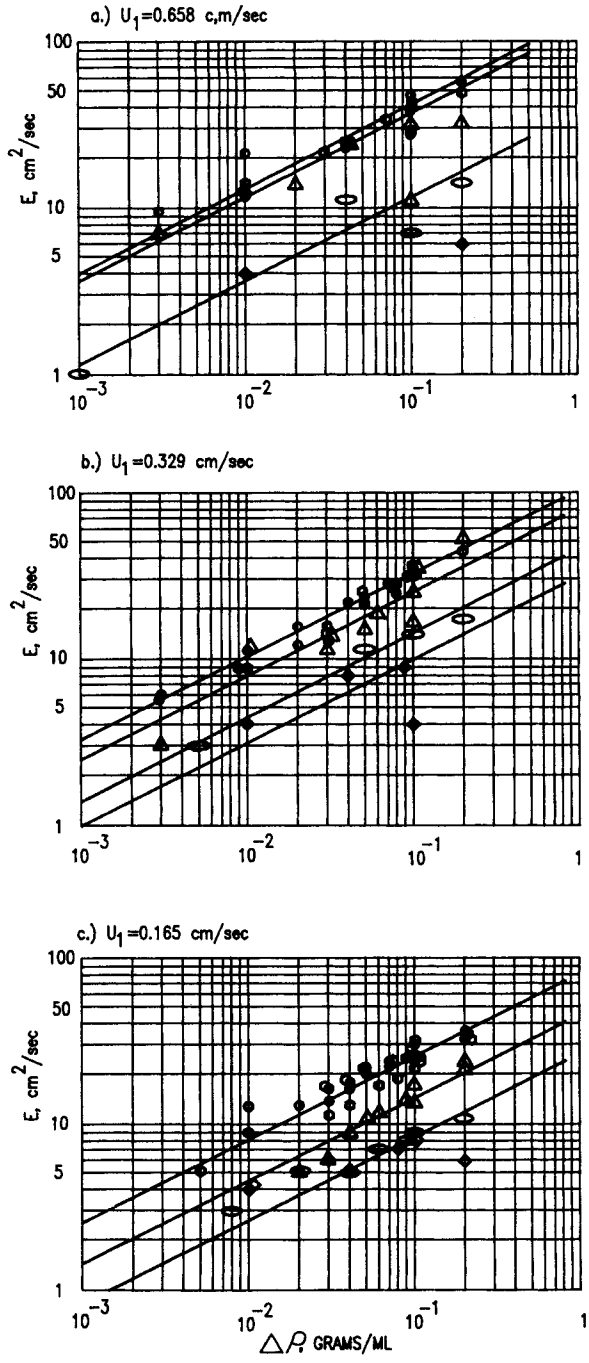

Figure 3. Effect of density difference on axial dispersion coefficient at different water superficial velocities, plate spacing 5.24 cm.

Agitation speed, rpm: 0 50 79 100 200 300
Symbol: o o □ △ ⬭ ◇

To illustrate the effect of water upflow velocity on E, the smoothed E values at 0 rpm, E_o, obtained from Figures 3 and 4, are plotted as a function of $\Delta\rho$ in Figure 5. It is interesting to note that as $\Delta\rho \to 0$ these E_o values approached 1-3 cm^2/s, the values previously mentioned for uniform fluids.

To illustrate the effect of agitation upon the axial dispersion coefficient, E/E_o values are plotted as a function of agitation frequency in Figure 6. With agitation, the axial dispersion

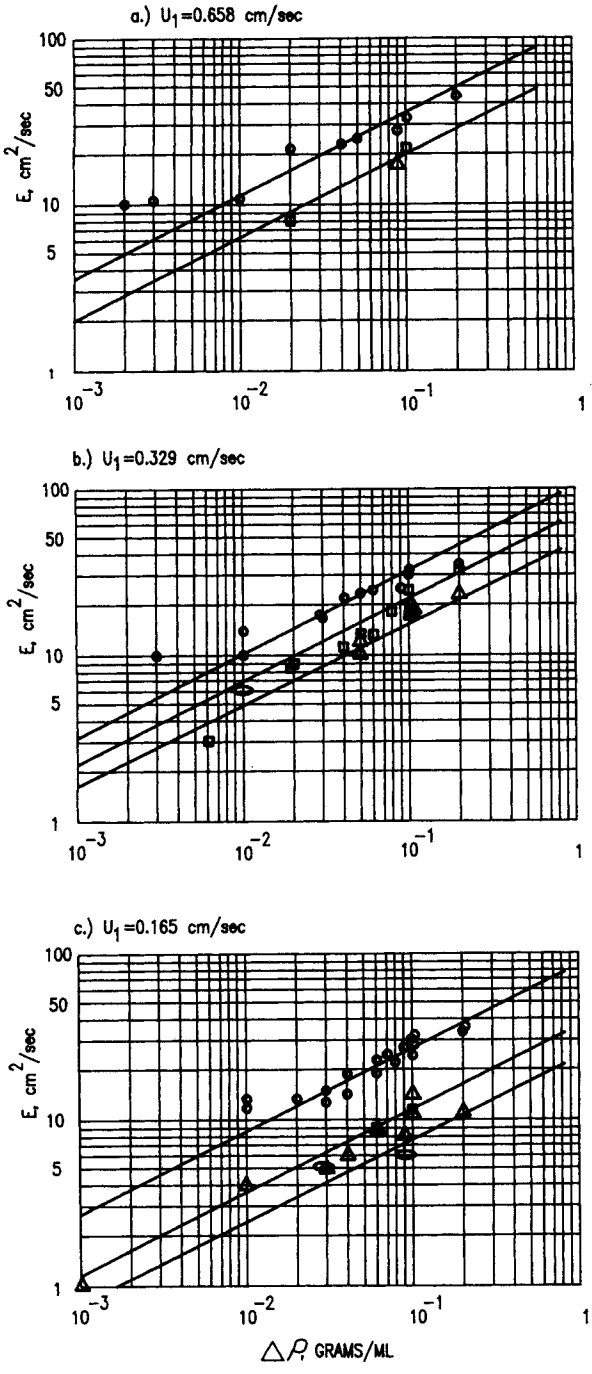

Figure 4. Effect of density difference on axial dispersion coefficient at different water superficial velocities, plate spacing 2.70 cm.

Agitation speed, rpm: 0 50 79 100 200 300
Symbol: o o □ △ ⬭ ◇

coefficients are reduced to approximately 30% of the non-agitated column E values. This reduction in axial dispersion coefficient is achieved faster with 2.7 cm plate spacing as compared to 5.24 cm spacing.

Effects of Buoyancy and Agitation on Axial Mixing

In the absence of agitation, axial dispersion coefficients may

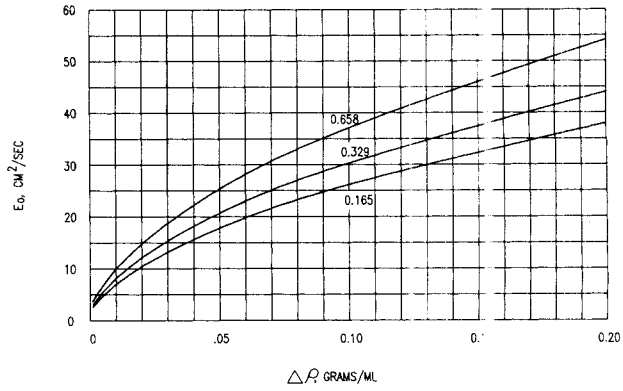

Figure 5. Effect of density difference on axial dispersion coefficient in the absence of agitation, for different values of water superficial velocity indicated in cm/s (smoothed curves).

be characterized as a function of the buoyant energy dissipation rate per unit mass, ϵ_b, defined as:

$$\epsilon_b = \frac{gU_1\Delta\rho}{\rho} \tag{9}$$

A plot of E_o vs. ϵ_b is shown in Figure 7. The straight line represents the following empirical correlation:

$$E_o = 9.32\epsilon_b^{0.347} \tag{10}$$

which fits the data with a standard deviation of 15.7%. The units of ϵ_b to be used in Eq. 10 are cm^2/s^3 (10^4 W/kg).

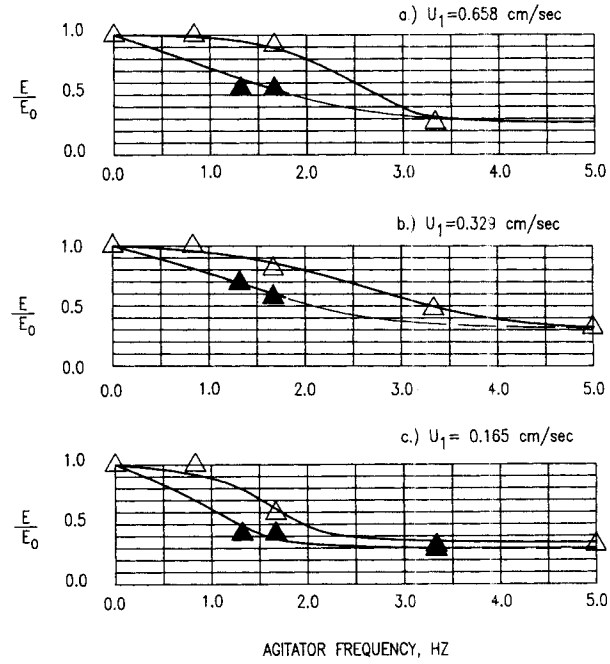

Figure 6. Effect of agitation frequency on ratio E/E_o for different water superficial velocities.

Plate spacing, cm: 2.70 5.24
Symbol: ▲ △

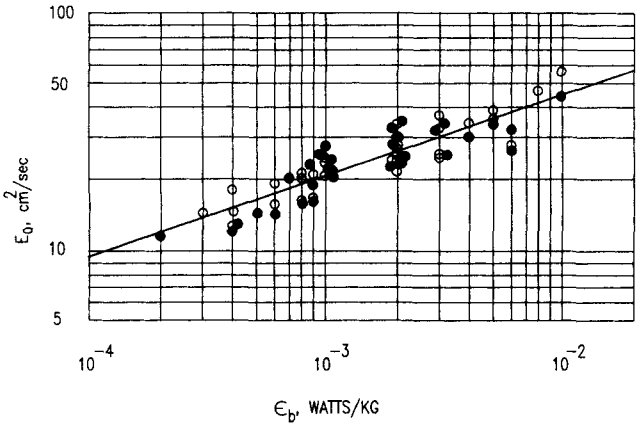

Figure 7. Correlation of E_o with buoyant energy dissipation.

Plate spacing, cm: 2.70 5.24
Symbol: ● ○

With agitation, both mechanical and buoyant energy dissipation rates per unit mass are important in characterizing E. As discussed by Hafez and Baird (1978), ϵ_m, the mechanical dissipation per unit mass may be defined as:

$$\epsilon_m = \frac{2\pi^2}{3}\left(\frac{1-S^2}{C_o^2 S^2}\right)\frac{(Af)^3}{h} \tag{11}$$

and total energy dissipation per unit mass is

$$\epsilon_t = \epsilon_b + \epsilon_m \tag{12}$$

Axial dispersion coefficients were correlated by multiple regression analysis to obtain the following equation:

$$E = 9.52\epsilon_b^{0.535}\epsilon_t^{-0.186} \tag{13}$$

A plot of $E/(9.52\epsilon_b^{0.535})$ vs. ϵ_t is shown in Figure 8. This correlation fits the experimental data with a standard deviation of 17.9%. For the case of $\epsilon_m \to 0$ Eq. 13 becomes

$$E_o = 9.52\epsilon_b^{0.349} \tag{14}$$

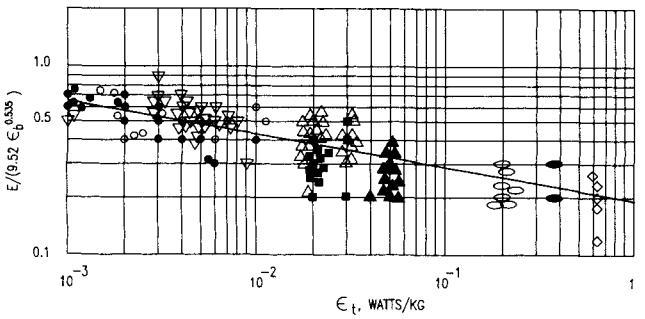

Figure 8. Correlation of E with buoyant and mechanical energy dissipation.

Agitation speed, rpm: 0 50 79 100 200 300
Symbols for $h = 2.70$ cm: ● ▼ ■ ▲ ⬬ ◆
Symbols for $h = 5.24$ cm: ○ ▽ ▣ △ ⬭ ◇

which is in reasonable agreement with Eq. 10. The ϵ_b and ϵ_t values to be used in Eqs. 10 and 13 have units of $cm^2 \cdot s^{-3}$ and the resulting E_o and E values have units of $cm^2 \cdot s^{-1}$.

Dimensional Analysis

The effect of variables upon E can be arrived at by dimensional analysis, assuming that E has a power-law relationship with gravity, the density gradient, dp/dz, the fluid density, and a mixing length term ℓ.

$$E \alpha g^p \left(\frac{d\rho}{dz}\right)^q \rho^r \ell^s \tag{15}$$

It is assumed that viscosity plays no significant part because the eddy sizes greatly exceeded the minimum eddy size estimated from energy dissipation. If it is further assumed that the density gradient term is coupled to g (i.e., $p = q$); then dimensional analysis shows that $p = q = 1/2$, $r = -1/2$, and $s = 2$. Hence,

$$E \alpha \ell^2 \left(\frac{g}{\rho}\cdot\frac{d\rho}{dz}\right)^{1/2} \tag{16a}$$

The mixing length term can be defined from the above equation such that

$$E = \ell^2 \left(\frac{g}{\rho}\cdot\frac{d\rho}{dz}\right)^{1/2} \tag{16b}$$

The above analysis gives E in terms of density gradient, but it can also be expressed in terms of the density difference $\Delta\rho$. From Eqs. 5 and 7, which assume a linear dependence,

$$\Delta\rho = 0.7c \tag{17}$$

Substituting in Eq. 1, we obtain

$$U\Delta\rho = E\cdot\frac{d\rho}{dz} \tag{18a}$$

Rearrangement gives:

$$\frac{d\rho}{dz} = \frac{U}{E}\cdot\Delta\rho \tag{18b}$$

Substitution of Eq. 18b in Eq. 16b and rearrangement gives:

$$E = \ell^{4/3}\left(\frac{gU\Delta\rho}{\rho}\right)^{1/3} \tag{19}$$

As noted previously, the term U is within 10% of the superficial water velocity U_1, so Eq. 19 is within 3% of the following relationship

$$E = \ell^{4/3}\epsilon_b^{1/3} \tag{20}$$

where ϵ_b is defined in Eq. 9.

The validity of this approach is confirmed by the closeness

of the best-fit exponent of ϵ_b of 0.347 in Eq. 10 to the predicted value of 1/3. Equation 10 also provides an estimate of the mixing length ℓ, which is approximately 5.3 cm in the absence of plate agitation. This value is about 70% of the column diameter and suggests the existence of large-scale eddies due to convective mixing.

The effect of plate agitation in reducing convective mixing can be interpreted in terms of a reduction in the mixing length term in Eq. 20. At an agitation speed of 5.0 Hz ($Af = 9.53$ cm/s), the present data indicate that the effective mixing length is approximately 2 cm. It is likely that the flow of an immiscible dispersed phase (liquid or gas) would also have some effect in reducing the mixing length from the large value observed in single-phase convective flow.

Conclusions

The following conclusions can be drawn about the 7.62 cm. dia. Karr column tested:

1. A large adverse density gradient in the continuous phase can result in increased axial mixing. If the overall density difference, $\Delta\rho$, is 0.2 g/mL, axial dispersion coefficients 10 to 20 times higher than those in uniform fluids have been observed with the $CaCl_2$ brine–water system.

2. Agitation reduces backmixing for concentration-gradient-induced axial mixing. At 300 rpm, E values were observed to be only 30% of E values at 0 rpm. The physical interpretation of this effect is that the supply of mechanical energy to the system reduces the eddy size (mixing length), thereby reducing axial mixing.

3. Several empirical correlations have been developed to characterize axial mixing due to adverse concentration gradients. For the case of no agitation, E correlates with buoyant energy dissipation per unit mass, with the exponent being close to that predicted from dimensional analysis. For the case with agitation, E correlates with both buoyant and mechanical energy dissipation per unit mass.

4. Further work on adverse density gradient effects is recommended to examine particularly the effect of column diameter, and the flow of a dispersed liquid phase. It is expected that convective mixing will increase with column diameter but will be reduced by the presence of a counterflowing liquid phase. Further work is needed not only on the reciprocating plate column but on other types of extraction columns. It is expected that convective mixing will be less with plates having smaller open areas.

Acknowledgment

The authors are grateful to the Otto H. York Company, Inc. for permission to publish this work. Presentations based on it were made at the International Solvent Extraction Conference, ISEC 90, at Kyoto, Japan, in July 1990, and at the 1990 Annual Meeting of the AIChE, Chicago, November 1990.

Notation

A = agitation stroke, cm
c = concentration, g/mL
C_o = orifice coefficient for perforated plates; 0.6 in this work
E = axial dispersion coefficient, $cm^2 \cdot s^{-1}$
E_o = axial dispersion coefficient in absence of agitation, $cm^2 \cdot s^{-1}$
f = agitation frequency, rpm or Hz
g = acceleration due to gravity, $cm \cdot s^{-2}$
h = plate spacing, cm
ℓ = mixing length, cm
L = plate stack height, cm
Pe = Peclet number defined as $(UL)/E$
p,q,r,s = exponents determined by dimensional analysis
S = plate fractional open area
U = superficial velocity, $cm \cdot s^{-1}$
U_1 = superficial velocity of water fed to the column, $cm \cdot s^{-1}$
z = vertical distance (upward direction), cm

Greek letters

ϵ_b = buoyant energy dissipation rate, W/kg or $cm^2 \cdot s^{-3}$
ϵ_m = mechanical energy dissipation rate, W/kg or $cm^2 \cdot s^{-3}$
ϵ_t = total energy dissipation rate, W/kg or $cm^2 \cdot s^{-3}$
$\Delta\rho$ = difference in density between continuous phase and pure water, g/mL
ρ = solution (continuous phase) density, g/ml
ρ_o = density of pure water, g/mL

Literature Cited

Hafez, M. M., and M. H. I. Baird, "Power Consumption in a Reciprocating Plate Column," *Trans. Inst. Chem. Engrs. (London)*, **56**, 229 (1978).

Hafez, M. M., M. H. I. Baird, and I. Nirdosh, "Flooding and Axial Dispersion in Reciprocating Plate Extraction Columns," *Can. J. Chem. Eng.*, **57**, 150 (1979).

Hartland, S., and J. C. Mecklenburgh, "A Comparison of Differential and Stagewise Countercurrent Extraction with Backmixing," *Chem. Eng. Sci.*, **21**, 1209 (1966).

Karr, A. E., "Performance of a Reciprocating Plate Extraction Column," *AIChE J.*, **5**, 446 (1959).

Karr, A. E., and T. C. Lo, "Performance and Scale-Up of a Reciprocating Plate Extraction Column," *Proc. Int. Solvent Extn. Conf. (ISEC 71)*, The Hague, 299, Soc. Chem. Ind., London (1971).

Karr, A. E., and T. C. Lo, "Performance of a 36-in. Diameter Reciprocating Plate Extraction Column," *Proc. Int. Solvent Extn. Conf. (ISEC 77)*, Toronto, **1**, 355, Can. Inst. Mining and Met., Montreal (1979).

Karr, A. E., S. Ramanujam, T. C. Lo, and M. H. I. Baird, "Axial Mixing and Scaleup of Reciprocating Plate Columns," *Can. J. Chem. Eng.*, **65**, 373 (1987).

Kim, S. D., and M. H. I. Baird, "Axial Dispersion in a Reciprocating Plate Extraction Column," *Can. J. Chem. Eng.*, **54**, 81 (1976).

Mar, B. W., and A. L. Babb, "Longitudinal Mixing in a Pulsed Sieve Plate Column," *Ind. Eng. Chem.*, **51**, 1011 (1959).

Miyauchi, T., and T. Vermeulen, "Longitudinal Dispersion in Two-Phase Continuous Flow Operations," *Ind. Eng. Chem. Fundam.*, **2**, 113 (1963).

Pratt, H. R. C., "A Simplified Analytical Design Method for Stagewise Extractors with Backmixing," *Ind. Eng. Chem. Process Des. Dev.*, **14**, 74 (1975).

Pratt, H. R. C., and M. H. I. Baird, "Axial Dispersion," *Handbook of Solvent Extraction*, T.C. Lo, M. H. I. Baird, C. Hanson, eds., Ch. 6, Wiley-Interscience, New York (1983).

Sleicher, C. A., "Axial Mixing and Extraction Efficiency," *AIChE J.*, **5**, 145 (1959).

Sleicher, C. A., "Entrainment and Extraction Efficiency of Mixer-Settlers," *AIChE J.*, **6**, 529 (1960).

Manuscript received Sept. 5, 1990, and revision received Dec. 27, 1990.

See NAPS document no. 04840 for 10 pages of supplementary material. Order from NAPS c/o Microfiche Publications, P.O. Box 3513, Grand Central Station, New York, NY 10163. Remit in advance in U.S. funds only $7.75 for photocopies or $4.00 for microfiche. Outside the U.S. and Canada, add postage of $4.50 for the first 20 pages and $1.00 for each of 10 pages of material thereafter, $1.50 for microfiche postage.